Revista Brasileira de Geofísica; 1987, Vol. 5, 73-90

doi: 10.22564/brjg.v5i2.2228

THE MATURATION OF GEOTHERMICS AS A DISCIPLINE AND SOME UNRESOLVED PROBLEMS

A.E. BECK

Department of Geophysics, University of Western Ontario, London, Canada N6A 5B7.

Some of the difficulties involved in the determination of heat flow density values (HFD) and of the associaded statistical estimate of their errors are reviewed. Particular attention is paid to the problems that arise when a local HFD, which may have narrow error bounds, is mistakenly accepted as a regional HFD, which may have significantly larger error bounds, and used to downward continue the temperature and heat flow field to lithospheric depths. Two aspects which are covered in some detail are the errors in determining equilibrium temperature gradients in boreholes or lake and oceanic sediments, and the errors which arise in thermal conductivity measurements when the thermal contact resistance, especially for porous rocks saturated with a low conductivity fluid, is mistakenly assumed to be negligible.

Algumas das dificuldades envolvidas na determinação dos valores de densidade de fluxo térmico (HFD) e das estimativas estatísticas de seus erros são revisadas. Uma atenção particular é dada ao problema que aparece quando um HFD local, que pode ter erro pequeno, é erroneamente aceito como um HFD regional, que pode ter erro significantemente maior, e é usado para continuar o campo de temperatura e de fluxo de calor a profundidades litosféricas. Dois aspectos que são discutidos em detalhe são os erros na determinação dos gradientes de temperatura em equilíbrio em furos e sedimentos lacustres ou marinhos e os erros que aparecem nas medidas de condutividade térmica quando a resistência térmica de contato, especialmente para rochas porosas saturadas com um fluido com baixa condutividade é erroneamente suposto como desprezível.

(Traduzido pela Revista)

INTRODUCTION

Knowledge of the distribution of heat sources and temperature within the earth, both now and in the past, is a fundamental requirement for a better understanding of many geophysical, geochemical and geological phenomena. The origin and history of the development of the earth, the formation of mountain systems and ocean basins, the origin of earthquakes and volcanoes are all intimately bound up with the availability and distribution of all forms of energy of which thermal energy is the most important and, when that thermal energy is near the surface it can be of great practical use.

The Greeks were the first to recognize and record a connection between earthquakes and volcanoes; this probably makes them the first geothermicists or first seismologists — certainly they were the first geophysicists. From the time of Anaximenes, Anaxagorus, Democritus and Aristotle there are written records of man's general interest in all natural phenomena but particulary in anomalous geothermal areas, such as volcanoes and hot springs, that interest being expressed in the form of theories (often with religious overtones) put forward to account for the existence of those phenomena. It was only when mines reached significant depths in the 16th and 17th Centuries that people became aware of a general increase of temperature with depth (Mairan, 1749). But it was not until the middle of the 19th Century that an attempt was made to obtain information on terrestrial heat in a systematic manner when the British Association for the Advancement of Science set up a committee for this purpose under the chairmanship of J.D. Everett. That committee produced a number of reports until close to the end of the 19th Century when interest dwindled until the 1930's; in that decade landmark papers were published by Benfield (1939), Bullard (1939) and Krige (1939) which mark the beginning of the modern explosion of interest in all aspects of geothermics. Initially, the interest was in the basic aspects of terrestrial heat but in the last two decades, probably starting with the first United Nations Conference, Rome 1970, there has been ever increasing interest in making use of the earth's natural thermal resources for space heating manufacturing processes and electricity.

The Need for Confidence in HFD Values

Now that attempts to fit the measured heat flow density (HFD) values to various hypotheses dealing with such things as the thermal history of the earth, sea floor spreading, plate tectonics, local and regional orogenic

activity, it is necessary to take a closer look at current techniques so as to be sure that the values we use are in fact valid for the region we suppose they represent and have not been rendered useless by purely local phenomena. One thing lacking in general is a method of obtaining reliable error bounds on the mean values. It is important that a universally acceptable method of calculating error by a reliable statistical technique be developed because when a HFD value is used to calculate temperatures and HFD at lithospheric depths, the manner in which the errors on near surface measurements are propagated whould accompany such calculations. The current general method of a set of forward calculations, often with intuitive bounds, is not sufficient; the range of errors found by such methods may be much too small.

The Basis of HFD Measurements

As is well known, when reference is made to HFD values only the conductive component of terrestrial heat transfer is implied; this is because the values are obtained by taking the product of a temperature gradient and a thermal conductivity.

We usually try to measure temperature gradients in a borehole from which a core has been extracted for thermal properties measurements in the laboratory. The first modern measurements using this technique were reported by Benfield (1939) and Bullard (1939) and were made in holes that penetrated to great depths (greater than a kilometer) and in regions that were relatively uncomplicated geologically. Equipment was heavy, and measurements took much time. Although later on efforts were made to take into account possible influences of topography, every effort was made to avoid regions where subsurface water flows were suspected. Similarly, with oceanic heat flow data the early measurements were very carefully planned to be in regions where effects of sedimentation and bottom temperature variations were negligible. The early results from both continents and oceans were so interesting and valuable that considerable effort was put into the development of more rapid techniques of measurement. And here we may have gradually slipped into a lower quality of field planning. We are in danger of losing sight of the fact that even if reliable, high quality data are relatively few in number, they are probably more valuable than vast quantities of unreliable low quality data. In this context we define a reliable HFD as one which has error bounds, narrow or wide, which have been determined by a generally accepted statistical analysis; a high quality HFD value is one with narrow reliable error bounds. After we have rigorously tested certain ideas and satisfied ourselves that in a particular situation our techniques produce accurate and reliable results, under all the pressures to produce large quantities of data quickly we have then without sufficient though transferred our techniques to situations where in fact something different should be done.

It is as well to point out that in reducing HFD determinations to the measurement of thermal conductivity and temperature gradient, the implicit assumptions in such a simplification are that heat transfer by mass movement is negligible, that contributions from heat sinks and heat sources are negligible, that the depth over which the measurements are made are negligibly small compared with the radius of the earth, that the area of interest is negligibly small compared with the curvature of the surface of the earth, that the surface of the earth is invariant (that is, it has not been subjected to geological processes), and that the temperature at the surface of the earth is time dependent; all these assumptions are based upon the view that the principal parameter of interest is not the local HFD but the regional, long term equilibrium HFD which in turn requires the assumption that the thermal regime of the earth is quasi-steady-state for periods of the order of the time constant for the curst — that is, a few hundred thousand to a few million years. It has, of course, been known for many years that these boundary conditions are not met and it is usual to apply appropriate corrections seriatum if enough is known about the departure of the true boundary conditions from those that have been assumed. Some of the techniques developed for handling the corrections are subject to question. For example, recent work by Powell et al. (1987) indicates that we still have a problem in producing reliable corrections for topographic effects. Since topographic corrections are really just a specialized form of structural corrections it may turn out that there is more to be learnt about corrections for structural effects as well.

Other effects to be born in mind are those of erosion and sedimentation. For example, erosion rates of 1mm per year over the last 1 million years will result in a 20% increase of the HFD values for material of typical diffusitivity $10^{-6}m^2s^{-1}$. On the other hand, sedimentation rates of 1mm per year over the same period will result in a 20% decrease of HFD values for material of the same diffusitivity, and 40% for materials of $0.2 \times 10^{-6}m^2s^{-1}$, a value that is quite reasonable for some continental lakes. If the sedimentation rate is particularly rapid, say 10 mm/year, the error would amount to 80-100%. These estimates do not take into account the effects that these processes have on the removal and addition of heat sources. Finally, even if we have no structure and the surface of the earth is a perfect plain not subject to sedimentation or erosion, we know that the surface is not at constant temperature; it experiences daily, yearly and longer period variations.

The discuss all the problem areas would require a book. Therefore discussion in this paper will concentrate on potentially significant sources of error which may be influencing our data because of too casual acceptance of criteria of reliability in two areas: (a) that if a T-z plot, or a Bullard plot, is linear within acceptable statistical limits (usually ± a few percent), then it is assumed that there have been no significant effects to the steady state subsurface thermal regime due to topography, structure, surface temperature variations, heat sources and sinks, or hydraulically

driven water flows, and (b) that there are no errors due to contact resistance in the devided bar or stack of desks apparatus not any induced convection in the line source techniques used for unconsolidated sediments.

PROBLEMS ASSOCIATED WITH SURFACE TEMPERATURE VARIATIONS

Right at the beginning of the modern era of heat flow density determinations, it was recognized that surface temperature variations might have a significant influence on the results (Anderson, 1934; Benfield, 1939). However, it was easy enough to show that the effects of the annual temperature variations became insignificant at depths of 20-30m in typical materials so that measurements below those depths would not need corrections for this perturbation. The only other known temperature variation of concern was that of the rise and fall of surface temperature during the retreat and advance of ice sheets. One of the big difficulties with this latter correction is knowing the amplitude of the surface temperature change. In the early days corrections were applied in a rather simplistic manner, Fig. 1(a). It was assumed that the temperature at the base of the ice sheet was the same as that of the pressure melting point of ice under the pressures exerted by the ice sheet; that means that for a sheet 1 or 2 km thick, the melting point is depressed to —1 or —2°C. The onset and retreat of ice sheet are, geologically speaking, sudden so that the corrections were made assuming an instantaneous change of temperature at the surface. Since we have some idea of the mean surface temperature in the warm period, combining this with the assumed depressed melting temperature it is possible to obtain a value for the amplitude V. However, this may not be correct in all cases since evidence from th St. Lawrence Lowlands in Canada (Crain, 1968) suggests that the temperature at the bottom of the ice sheet during the last ice age was 4 or 5° lower than the pressure melting point, and temperatures of —13°C have been measured at the bottom of the Greenland ice sheet (Hansen & Langway, 1966).

The times for the ice sheet correction are, of course, very long — of the order of several thousands of years. Therefore, although the perturbations may have penetrated deeply, from one to several km, the amplitudes of the perturbations are highly damped and errors in HFD arising from incorrect assessment of this cause may not amount to more than 20-30%, especially in relatively shallow holes where the net effect is a temperature offset with little change on the gradient. As indicated in Fig. 1(a) it was usual to assume that amplitude of change during advance and retreat of a sheet was the same;this simplified the mathematics but as Figure 1(b) shows, it is quite easy to model practically any surface temperature change by a series of step changes (Beck, 1977a). In fact, a sinusoidal temperature change could be modelled by an appropriate series of step changes; alternatively, Fourier series techniques can be used to model sudden changes by a group of harmonic changes; the reason for choosing one over another is usually convenience.

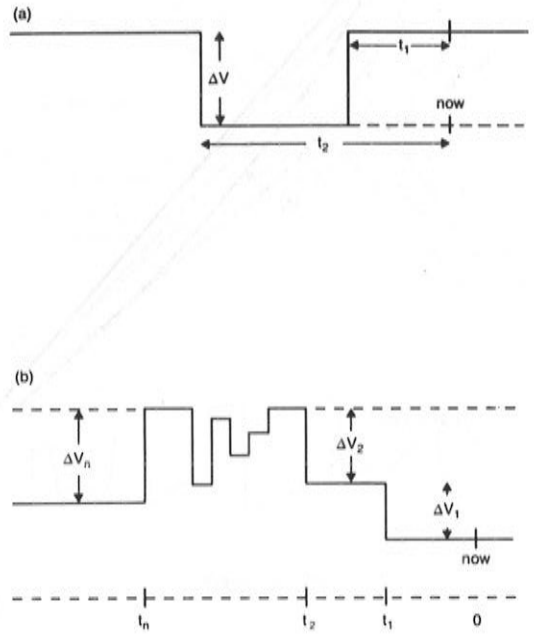

Figure 1. Models of surface temperature changes and their subsurface effects. T(z) is temperature at depth z, T_0 is mean surface temperature, α is thermal diffusivity, $\Gamma(z)$ is normal geothermal gradient, $\Delta\Gamma(z)$ is perturbation to normal gradient.

(a) Simple advance and retreat of an ice sheet.

$$T(z) = T_0 + \Gamma(z) - \Delta v[\mathrm{erf}(z/\sqrt{4\alpha t_1}) - \mathrm{erf}(z/\sqrt{4\alpha t_2})]$$

$$\Delta\Gamma(z) = [\Delta v/(\pi\alpha t_1)^{1/2}][\exp(-z^2/4\alpha t_1) - (t_1/t_2)^{1/2}\exp(-z^2/4\alpha t_2)]$$

(b) More complex model of surface temperature changes.

$$T(z) = T_0 + \Gamma(z) + \sum_{n=1} \Delta v_n \,\mathrm{erfc}\,(z/\sqrt{4\alpha t_n})$$

$$\Delta\Gamma(z) = \sum_{n=1} -\Delta v_n(\pi\alpha t_n)^{1/2}\exp(-z^2/4\alpha t_n)$$

Heat Flow Density Measurements in Boreholes

Fig. 2 illustrates in general terms what happens when a steady state regime, line 1, is perturbed by an instantaneous change, and a later recovery, of temperature a the surface. After a long time the T-z plot is curved, line 6, and the gradient is therefore a function of depth. The curvature in the figure is greatly exaggerated; in practise the curvature would frequently go undetected and it is here that we run into the first problem. What does this subtle curvature do to our determination of the temperature gradient and to the estimate of error in the gradient?

Fig. 3 shows a T-z plot for a typical PreCambrian Shield region which has a gradient of 15 mK/m; also shown are the 20% error bounds on the gradient. The crust is assumed to be completely homogeneous. If this temperature regime has been perturbed recently, in the last 1,000-2,000 years, by the form of surface temperature change, also shown on Fig. 3, representing the little ice age (Beck, 1977a) then the T-z plot obtained new would be as shown by the points. Curvature in the upper 150m can easily be seen and a good observer

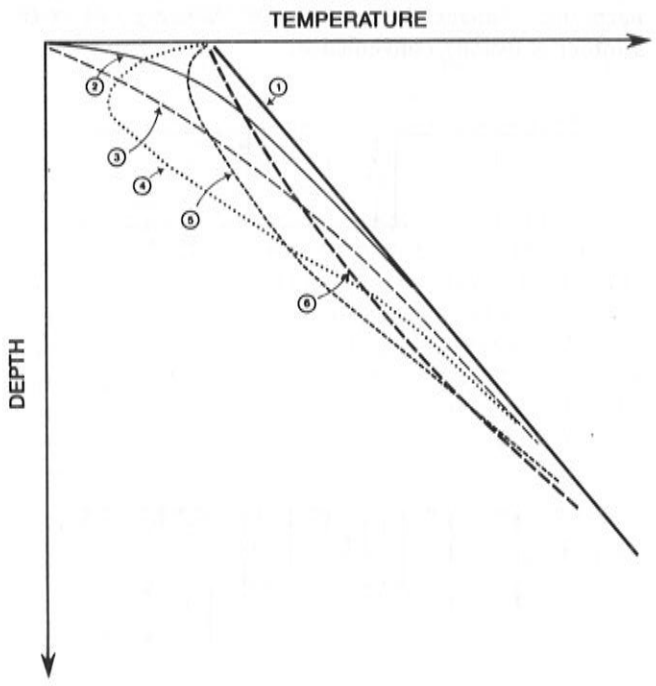

Figure 2. Schematic of variation of T-z profiles after a surface temperature change of the type shown in Figure 1(a). A specific depth scale is deliberately omitted because the effects illustrated are perfectly general, the only differences being that as the time since the step change increases the depth scale will increase. Soon after the changed temperature the T-z plot is as shown by line 2; later on, as the perturbations propagate into the medium the T-z plot would appear as in line 3. If the temperature suddenly increases again (in an ice age that means that the ice sheet retreats), then shortly after that change the T-z plot looks something like line 4; later on it would appear as line 5. After a very long time, the profile would look like line 6.

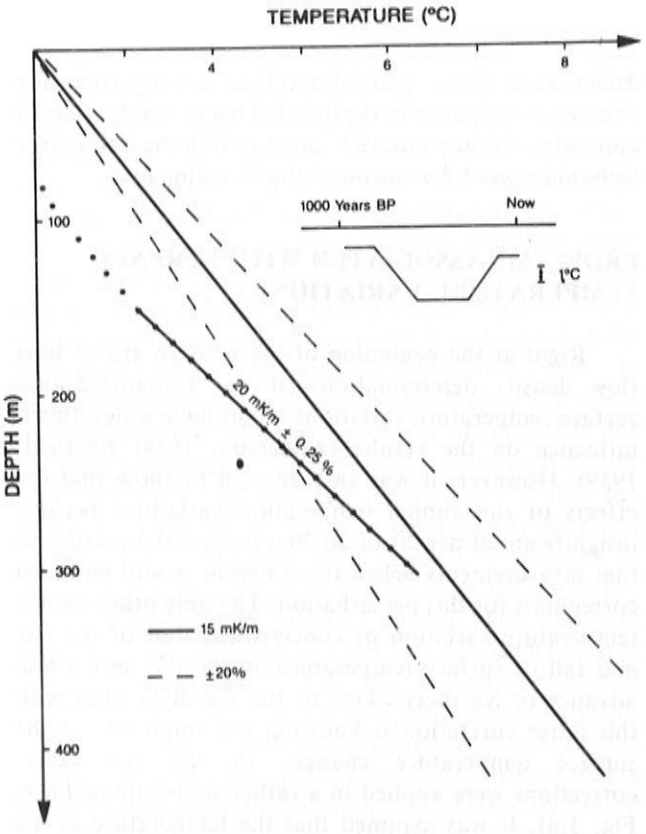

Figure 3. Steady state T-z plot, solid line through z = 0, with gradient of 15 mK/m and 20% error bounds (————); perturbed by surface temperature variation, shown as inset, to give perturbed T-z plot shown by points. Least squares straight line fit to points from 150-300m give a slope of 20 ± 0.25% mK/m.

would probably ignore this, and fit a least squares straight line through the group of points from 150-300m to obtain a gradient of 20 mK/m with a statistical coefficient of variation of <1%. This gives a false sense of security since the gradient is over 20% in error relative to the equilibrium value. Similarly, if we have a hole that was 450m deep and take the 300-450m section we get a gradient of 17 mK/m (+0.6%) — a 12% error in the equilibrium gradient. Fig. 3 refers to a completely homogeneous material where systematic curvature can be seen; however, if there are variations of thermal properties with depth of the type found in nature, i.e. some geological noise is added, the curvature would be impossible to pick up — even some of the curvature in the upper 150m might be difficult to see. Curvature due to any cause may be difficult to identify even if the gradient is plotted vs. depth using data obtained with newly developed high precision continuous logging equipment (Beck, 1982).

Therefore if reliable heat flow density values are to be obtained from relatively shallow boreholes in the continental crust, say 200-500m deep, details about the local climatic conditions over the last several hundred to a few thousand years must be known; the shallower the borehole we use the more important are the more recent, and more local, surface temperature variations. This leads to the problem of obtaining HFD from measurements in lake and offshore sediments.

Heat Flow Density Measurements in Lake Sediments

The advantages and disadvantages of the continental and oceanic methods are summarized in Table 1. For the reasons shown, but particularly because of the relative cheapness and ease with which one can make many measurements over a wide region using relatively shallow penetrating probes, there have been a number of attempts in the last decade or so to use the oceanic technique in the sediments of continental lakes. It was recognized at the outset that the temperature variations at the bottom of a lake would be much more significant than temperature variations at the bottom of oceans in the Abyssal Plains. Early experiments made use of lake bottom temperatures measured in small lakes and applied them to large (Hart & Steinhart, 1965), mean values from a group of lakes

were applied to individual lakes (Haenel et al., 1974), site monitor records which turned out to be too short were made (Allis & Garland, 1976, 1979; Beck, 1980). Later, very careful and detailed measurements in some European lakes (Lindqvist, 1984; Finckh, 1981) were made over several years leading to more confidence in the corrections that had to be applied but even here it appears that significant errors can arise if we do not pay attention to the details and take all influences, including structure, into account.

Table 1 – Advantages and disadvantages of continental and oceanic heat flow techniques.

Continents	
Advantages	**Disadvantages**
Deep penetration.	High cost of drilling – leads to limited choice of sites.
Possible detailed conductivity log.	Thermal disturbances persist for a long time.
Detailed T-z log.	
Oceans	
Low field costs – leads to possibility of many measurements in a small region.	Shallow pentration.
Thermal disturbance due to technique is relatively small.	Possible transient effects due to recent thermal events.
	Poor detail on λ and T-z logs.

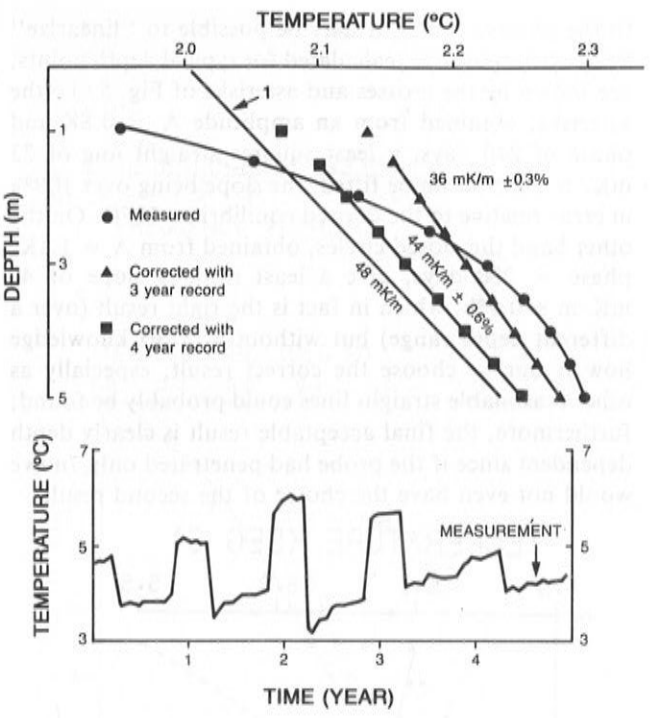

Figure 4. Steady state T-z profile in lake sediments, line 1, perturbed by 5 years of bottom temperature variations (BTV), inset, to give perturbed T-z profile shown by when measured at time shown by arrow. If • are corrected using only 3 years or 4 years of BTV results would be as shown by ▲ and ■ respectively.

To isolate the errors that arise from uncertainties in bottom temperature variations (BTV) a real bottom temperature variation is applied to a completely homogeneous medium. The series of temperatures was obtained in a shallow (about 30m deep) dimictic lake (Lindqvist, 1984). A long term steady state T-z profile is shown in Fig. 4; the perturbed profile due to the five years of BTV is shown by solid circles; i.e. if we measured temperatures vs. depth at the indicated point in the time series, we sould obtain a profile that passes through the • points. In other words, if we have the complete time series of measurements and use it to apply corrections to the measured data we would recover line 1. If we had only the last 3 years of measurements — and used them to apply corrected measurements we sould obtain the points indicated by triangles and fitting a straight line to the lower few meters would give what most observers would accept as a precise value for the temperature gradient but it is 25% in error relative to the desired equilibrium gradient. If 4 years of data were available, the corrected value would be closer to the desired value but although there is a statistically calculated coefficient of variation of less than 1% the gradient is in fact 10% in error.

For a one time probe measurement the importance of having long records of bottom temperature variations cannot be overemphasized; this implies many years of preliminary work monitoring temperatures at the sediment-water interface and there are no short cuts as the next example shows.

On a number of occasions there are no records of bottom temperature variations at all but there may be records, perhaps excellent records, of air and ground temperature variations from a nearby meteorological station. Clearly, the air temperature variations several tens of kilometers away, or even close to the lake, will not be identical with the temperature variations at the bottom of the lake — there will be differences in both amplitude and phase. Therefore, it might be argued, (Francheteau et al, 1984) if we have curvature in our T-z plot in the sediments and no variation in thermal properties, then any curvature is caused by BTV which can be corrected by assuming that the T-z profile should be linear and it is therefore justifiable to use a trial and error technique to adjust the amplitude and phase until the T-z plot becomes linear within an acceptable error limit. The problems are illustrated in Figure 5 which shows, dotted line, the steady state T-z profile in a homogeneous half space, the gradient being 48 mK/m. If the sediment surface has been subjected to BTV of the type and duration shown by inset (a) the T-z profile determined at end of the series would be as shown by line 2 of (a). However, if there are no BTV records, all that is known from the curvature ofline 2 is that the steady state profile has been perturbed. From other data, e.g. meteorological records, it might be known, or guessed, that the dominant perturbing period is annual (P = 1 year) and we guess at an amplitude (1 K in the present example). By trial and error varying of the amplitude and phase and applying them as corrections

to the observed data, it may be possible to "linearize" line 2; two solutions, calculated for typical depth points, are shown by the crosses and asterisks of Fig. 5. To the asterisks, obtained from an amplitude A = 0.8K and phase of 240 days, a least squares straight line of 23 mK/m ± 2.5% can be fitted, the slope being over 100% in error relative to the desired equilibrium HFD. On the other hand the closed circles, obtained from A = 1.1K, phase = 200 days, give a least squares slope of 48 mK/m ± 0.3%, which in fact is the right result (over a different depth range) but without a priori knowledge how is one to choose the correct result, especially as other reasonable straight lines could probably be found; furthermore, the final acceptable result is clearly depth dependent since if the probe had penetrated only 7m we would not even have the choice of the second result.

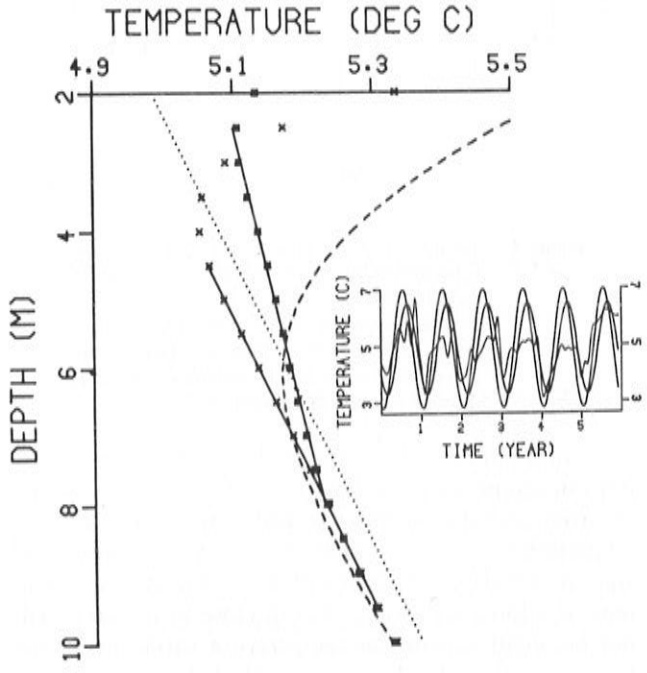

Figure 5. Steady state T-z profile (.....) giving a gradient of 48 mK/m perturbed byu six years of BTV shown as inset (a) to give a measured T-z profile of (-.-.-.). If the perturbed profile is corrected by trial and error variation of phase and amplitude until linear segments are obtained, two solutions (shown inset) would give T-z profiles shown by (*) and x which give gradients of 23 ± 0.3% mK/m respectively (after Wang et al, 1986).

So far the examples have been designed to illustrate the problems of BTV alone. To illustrate the problems that may arise if thermal properties structure is ignored, a real case from Lac Leman is taken (Finckh, 1981), Fig. 6. Finckh argued, as most would argue, that since the lowest 4 or 5 points show reasonable linearity and the upper points are clearly perturbed temperatures, it would be satisfactory to fit a straight line through only those points, and use a mean conductivity from the structure to arrive at a mean HFD value of 55 mW/m². However, as can be seen from (b), there is considerable power in the long period spectrum and if the measured points (x) are corrected for the complete 6 year time series of BTV and, assuming constant thermal properties in the sediments, the corrected T-z data give the open circles. However, the complete picture is even more complicated since if the conductivity structure is taken into account correcting the measured T-z points gives the plus (+) points. By trial and error we find a steady state HFD value of 109 mW/m² fits the corrected (+) data points used from 2-9m the solid line 2 being the steady state T-z profile. In figure form there does not appear to be much difference between the (o) and (+) points: the differences can be more clearly seen by referring to Table 2; all values being for the situation prior to any additional corrections for sedimentation, topography, etc. is the original value. (b) shows the HFD obtained from a Bullard plot using mean conductivity down to the maximum depth shown; the penultimate column is the heat flow value that would result, and the last column shows the coefficient of variation, over the depth ranges indicated, 5-9m for direct comparison with (a) and (c), 2-9m for along probe and 1-4m for a short probe. It is clear that a short probe would give very different results than would be obtained using longer probe, although from the coefficient of variation this might not be suspected. (c) is similar to (b) except that now allowances have been made for the

Table 2 – Effect of conductivity structure on HFD values from lakes.

(a) Original value assuming perturbation from BTV of Fig. 7(a) is negligible over 5 – 9m and with a constant conductivity equal to the harmonic mean of the observed conductivities (Fig. 7c) to the greatest depth in the depth range.

(b) After correcting for BTV and with same assumptions about conductivity as in (a) and using Bullard (1939) plots ($T_z = T_o + H \Sigma (\Delta z/\lambda_{mean})$.

(c) After correcting for BTV using the complete conductivity structure of Fig. 7a and Bullard plots ($T_z = T_o + H \Sigma (\Delta z/\lambda_z)$.

H and error values in brackets are results which would be obtained if harmonic mean conductivity of whole 9m section is used.

	Depth range (m)	λ ($W m^{-1} K^{-1}$)	H $mW m^{-2}$	Coefficient of variation (%)
(a)	5 – 9	1.46	55	3
(b)	5 – 9	1.46	90	2
	2 – 9	1.46	105	5
	1 – 4	1.20	106	6
(c)	5 – 9	Structure	109	3
	2 – 9	Structure	111	2
	1 – 4	Structure	127	3

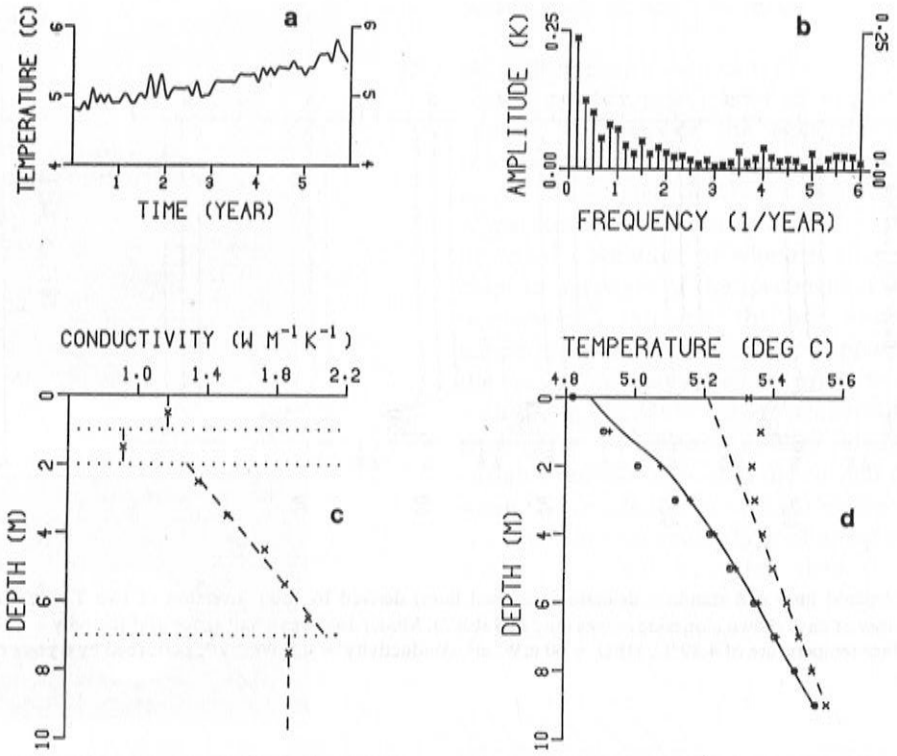

Figure 6. Data pertaining to Lac Leman. (a) Recorded water BTV. (b) Amplitude spectrum of the BTV in (a) (mean temperature, i.e., constant bias has been removed). (c) "x" points show measured conductivity values; dashead line is the conductivity model used in calculations. (d) Original and recalculated profiles. Crosses (x) are the measured temperatures at depths shown. Dashed line (————) is the original steady state profile, giving a heat flow value of 55 mWm^{-2}. "o" represent corrected temperatures using a constant conductivity model where λ = 1.46 W m^{-1} K^{-1} is the harmonic mean of the observed conductivity values over 0-9m as shown in (c). "+" represent corrected temperature data using the four-layer model in (c) and the surface temperature record in (a). The "best fit" steady state temperature profile from 1-9m with the conductivity model in (c) is shown by the solid line and gives a heat flow value of 109 mWm^{-2}. The Bullard plot gives 113 ± 3%.

details of the thermal properties structure rather just assuming a mean value for the whole sequence. To appreciate the effect of ignoring structure, values over the same depth ranges in (b) and (c) should be compared. In other words, even if there is complete control of BTV, errors of 20% can arise if the details of the variations of thermal properties with depth are not taken into account.

Therefore, to obtain a reliable HFD value from a one time single site set of measurement, several years of BTV measurements are needed.

This particular problem may be overcome with a technique that makes use of more than one T-z profile from a single site, separated in time by 1/4 to 1/2 of the period of the principal BTV. These profiles are jointly inverted using known a priori values of the various

Table 3 — A posteriori HFD and T_0 obtained by joint inversion of two T-z plots separated in time by (n — 1) months. The input a priori values of HFD and T_0 are 90 ± 100 mV m^{-2} and 4.5 ± 0.5°C, respectively, in all cases; a priori BTV is set to zero and all the other parameters are accurately known. True values of HFD and T_0 are 60mWm^{-2} and 4.89°C respectively.

n	Profiles used	Separation (days)	A Posteriori HFD (mWm^{-2})	T_0(°C)
1	1 only	–	24.0 ± 23.2	5.11 ± 0.18
2	1,2	30	44.8 ± 17.9	4.98 ± 0.15
3	1,3	60	55.1 ± 14.7	4.90 ± 0.13
4	1,4	90	61.0 ± 13.4	4.86 ± 0.12
5	1,5	120	61.4 ± 12.8	4.86 ± 0.12
6	1,6	150	59.5 ± 12.7	4.87 ± 0.11
–	All 6		62.4 ± 10.1	4.86 ± 0.10

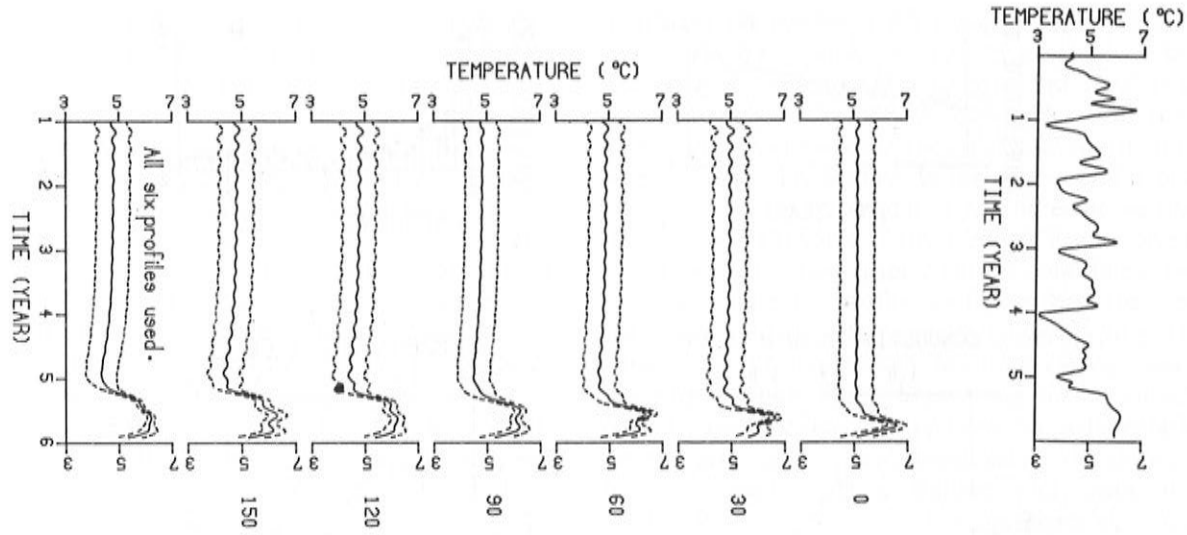

Figure 7. BTV (solid line) and standard deviations (dashed lines) derived by joint inversion of two T-z profiles separated by number of days shown alongside curves (and in Table 3). Model used was a half space of diffusivity = 0.225 mm^2s^{-1}, mean surface temperature of 4.89°C, HFD = 60 mW/m^2, conductivity = 0.8 $Wm^{-1}k^{-1}$, perturbed by 6 years of BTV shown at top.

parametes together with their variances, large if they are poorly known (e.g. the HFD) and small if they are well known (e.g. the temperatures), to obtain posteriori maximum likelihood values and variances of those parameters and the previously unknown and unmeasured BTV. The technique is still being developed (Wang & Beck 1987) but is illustrated using a simple model in Figs. 7 and Table 3. It can be seen from the table that the standard deviation on the HFD steadily decreases until about 3 months separation of two profiles after which HFD value is close to the true value but the coefficient of variation is about 20% although reasonably stable. From Fig. 7 it can be seen that the standard deviation for the early years is large but that it decreases considerably for the most immediate year. If for more detail is required for the early years then more sets of measurements separated by greater times are required; if more detail is required of the BTV over the year immediately preceding the last measurement then more than two T-z profiles during the preceding several months are required.

Spaces does not permit an answer to the two further important questions "Even if we have an absolutely reliable HFD value from a 10m section of sediments, what does it mean? Over how large a region is it valid to within, say, 10%?"

Table 4 – Typical thermal resistances of contact film. λ in $W\,m^{-1}\,K^{-1}$, R in $10^{-5}\,K\,W^{-1}$ Compare with 1cm thick fresh quartzite ($\lambda = 7.1$) of $R = 141$.

Rock	Film Thickness $\ell(\mu m)$	Contact Film Material Water ($\lambda = 0.59$)	Oil ($\lambda = 0.12$)	Air ($\lambda = 0.025$)
Igneous	10	1.7	8	40
Sedimentaru	30	5	24	120

THERMAL CONDUCTIVITY PROBLEMS

Although there have been a few attempts to develop methods for measuring thermal conductivity in situ in boreholes (Beck et al., 1956; Beck et al., 1971; Villinger, 1983), far and away the most used techniques are the steady state divided bar or stack of discs methods (Benfield, 1939; Birch & Clark, 1940, Beck, 1957) for cored rocks and the transient cylindrical ("needle") probe technique for unconsolidated oceanic and lake sediments (Von Herzen & Maxwell, 1959). In the commonly used techniques there are still potential sources of systematic error which need further consideration if reliable HFD's are to be routine.

As is well known, in a typical laboratory experiment for determining the thermal conductivity of a specimen of rock, relatively small specimens have to be used and a thermal contact resistance is introduced between the surfaces of the specimen and the source of heat (and the temperature sensing devices); this thermal resistance can be significant. What is not so clearly recognized is the fact that the contact resistance really consists of two components; the first is due to the macroscopic misfit of the surfaces of the specimen and apparatus, Fig. 8(a), and the other is a granular contact resistance caused by the introduction of a macroscopic surface with a large radius of curvature (a flat surface being of infinite radius) compared with the radii of the grains (Fig. 8(b)). When specimens are prepared, particularly granular types that are weakly welded, whole grains and even clusters of grains can be knocked out of the surface leaving holes that must be filled by the saturating and contact fluid.

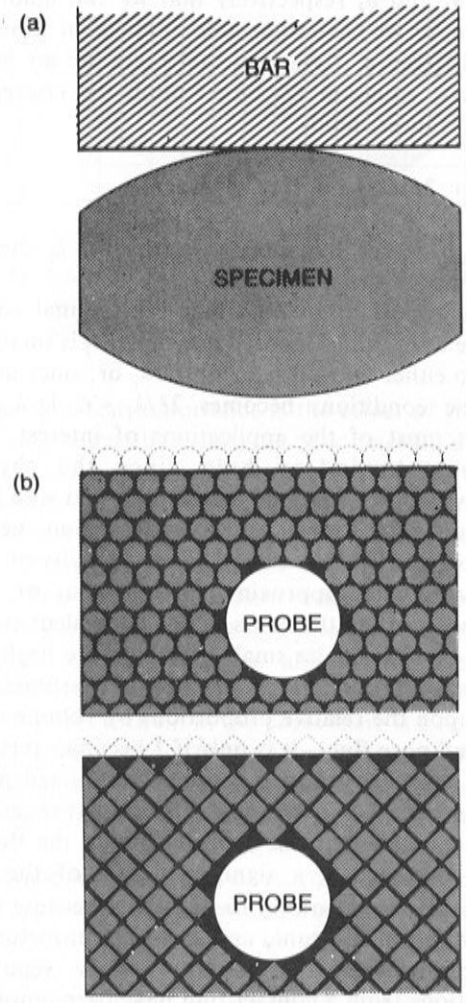

Figure 8. (a) Contact resistance due to misfit of two macroscopic surfaces. (b) contact resistance due to extra voids (unshaded areas) created when surface of large radius of curvature is introduced into a medium containing grains of small radius of curvature (after Beck, 1977b).

All other things being equal, the magnitude of the granular contact resistance will depend upon the grain shape as well as grain size. In Fig. 8(b) the diameter of the spherical grains of the top specimen is equal to the sidelength of the rounded cube grains in the bottom specimen and the darkened areas around the probe and at the surface represent the extra voids created which, due to the granular nature of the material, become the contact resistance. Ideally, one would like to be able to slice through th grains so that the surfaces as shown at the top of both types of material would not have the extra voids caused by grain plucking; for igneous and metamorphic rocks the spheres and cubes pictured as grains could represent crystals of the various minerals and frequently it is possible to slice throught them so that the surfaces are less pitted than in the case of sedimentary specimens, e.g. see bottom surfaces of specimens. For this reason, the contact resistances for igneous rocks are generally less than those for soft sedimentary rocks.

Steady State (Linear) Methods

Fig. 9 shows various types of equipment that have been used. The principle of all of them is the same — namely, to measure the heat flowing through the specimen at the same time as the temperature difference across a specimen of known thickness is determined. Apparatus (a) is a guardring type of apparatus, the principal advantage of which is that one can tolerate chips in the edges of the specimens if they occur during preparation. (a) and (b) are known as constant temperature difference types of apparatus, the ends of the bars being maintained at two different temperatures with the upper at the higher temperature; the electrical analogy is a constant voltage maintained across a variable resistance, so that the current (heat flow) varies when the resistance (specimen) changes. Apparatus (c) is a constant heat source type of apparatus, the electrical analogy bein that the current (heat flow) is constant so that as the resistance changes the voltage across the ends of the apparatus changes.

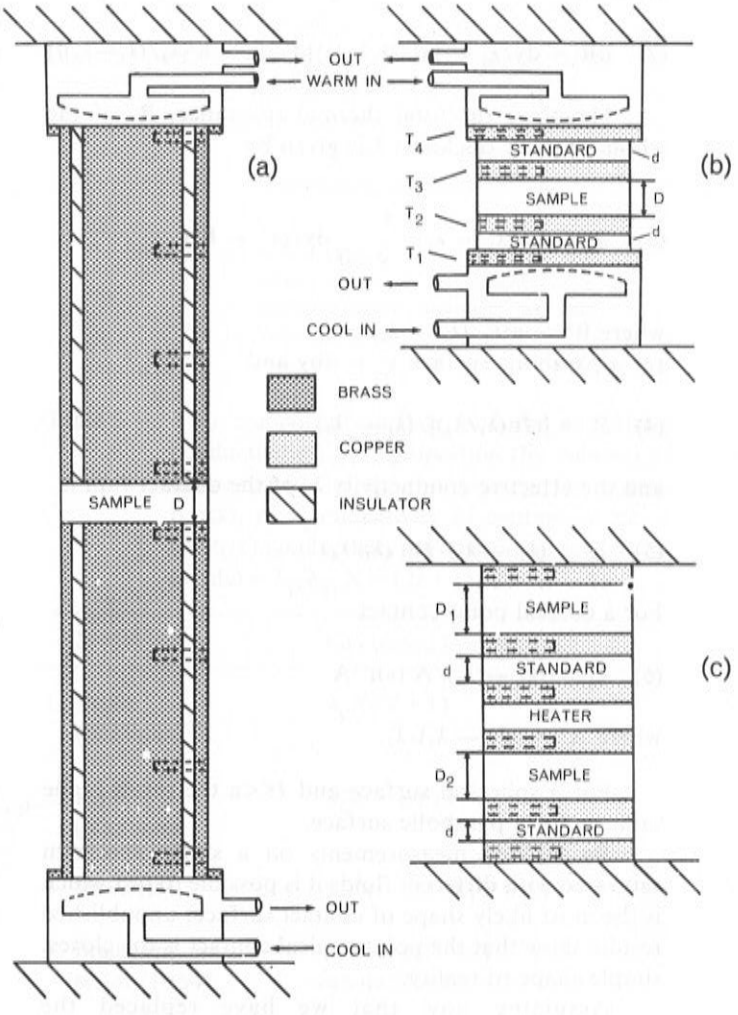

Figure 9. Three basic types of steady-state conductivity apparatus. (a) Guard ring constant temperature difference bar; (b) constant temperature difference stack of disks; (c) constant heat source, absolute type stack of disks.

We can determine the heat down the stack by measuring the temperature gradient along the bar, or across a disk, of known conductivity. If water is used as a contact fluid the contact resistance between the standards and the copper plates containing the temperature sensors is usually ignored; in many cases this does not lead to sensible error, but in other cases the error can be significant.

In all cases it is normal to take the complex geometry of a real contact surface and idealize it according to Fig. 10; it is soon found that the contact resistance appears to depend on the conductivity of the contacting surfaces. The reason for this can be demonstrated by referring to Fig. 11. An infinitesimally thin section of the contact film region is a disk, radius x, in parallel with an annulus of the contact fluid of outer radius a and the effective thermal conductivity, λ_e, of the section is given by

$$(1)\quad a^2\lambda_e = x^2\lambda_1 + (a^2 - x^2)\lambda_2$$

so that the elemental thermal resistance, dR, of the section is

$$(2)\quad dR = dy/\lambda_f = [a^2/(\lambda_1 - \lambda_2)]dy/[x^2 + a^2\{\lambda_2/(\lambda_1 - \lambda_2)\}]$$

Therefore the total thermal resistance, R, of the whole filme of thickness ℓ is given by

$$(3)\quad R = a^2/(\lambda_1 - \lambda_2) \int_{y=0}^{t} dy/(x^2 + B^2)$$

where $B^2 = a^2\lambda_2/(\lambda_1 - \lambda_2)$
for a parabolic surface $x^2 = 4by$ and

$$(4)\quad R \rightarrow [t\ell n(\lambda_1/\lambda_2)]/(\lambda_1 - \lambda_2)$$

and the effective conductivity λ_f of the contact film is

$$(5)\quad \lambda_f = (\lambda_1 - \lambda_2)/\ell \ln (\lambda_1/\lambda_2)$$

For a conical point contact

$$(6)\quad \lambda_f = (\lambda_1 - \lambda_2)/A \tan^{-1}A$$

where $A^2 = (\lambda_1 - \lambda_2)/\lambda_2$.

For a spherical surface and $\ell << a$ the result is the same as for a parabolic surface.

By making measurements on a single specimen saturated with different fluids it is possible to test which is the most likely shape of contact surface; unpublished results show that the point conical contact is the closest simple shape to reality.

Assuming now that we have replaced the complicated geometry of the contact region, Fig. 10(a), with the simplified series arrangement of Fig. 10(b), it can be seen that we really need to determine θ_3 and θ_2 to find ΔT, whereas in practice we can only determine T_3 and T_2. Somehow we have either to make T_3 and T_2 so close to θ_3 and θ_2 respectively that we can ignore the difference, or we have to be able to make an allowance for the difference. Assuming that there are no lateral heat losses, equation (7) based upon the concept of series resistances, holds

$$(7)\quad (D + 2\ell)/\lambda_{app} = (2\ell/\lambda_f) + D/\lambda_t$$

where λ_{app} is the apparent conductivity, λ_t the true conductivity of the specimen.

It is important to note that the thermal contact resistance term can be ignored only if $2\ell/\lambda_f$ is small with respect to either $D + 2\ell/\lambda_{app}$ or D/λ_t or, since usually $D >> \ell$ the conditions becomes $2\ell/\lambda_f << D/\lambda_{app}$ or D/λ_t In most of the applications of interest, these conditions do indeed hold since the thermal conductivity of the material is usually found with water as the fluid in the pores, and contact region, because that is how it exists in nature. The conductivity of water is relatively high (approximately half that of fused silica) and care the thickness of the equivalent contact film can be made quite small and therefore negligible. The thermal properties of the porous specimen also depend upon the relative proportions by volume of the matrix and pore fluid. It is only if ℓ becomes relatively large (as may happen in a very coarse grained poorly welded sediment) or λ_f becomes small (as in the case of a gaseous contact) that the contribution of the thermal contact resistance is a significant part of the total resistance. It is all too easy to think that because a film is thin, it is unimportant, and there are unfortunately many examples in the literature where significant contributions from a contact film have been ignored.

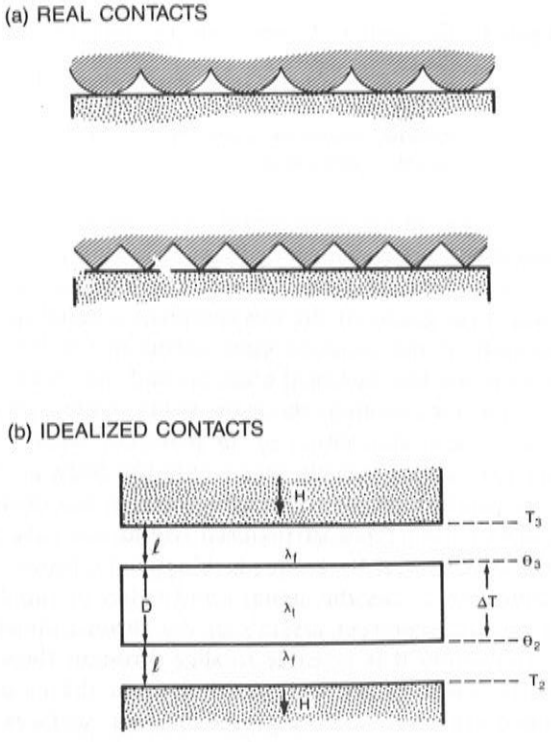

Figure 10. (a) Schematic of real contact surfaces. (b) Idealized equivalent of (a).

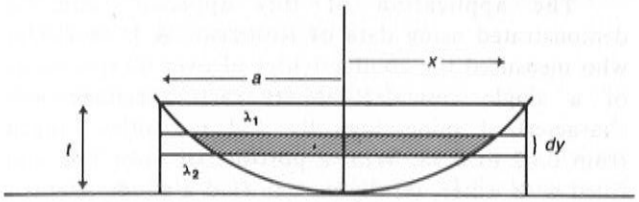

Figure 11. Schematic for deriving relations showing why thermal contact resistance depends on conductivities of contacting surfaces as well as conductivity of contact film.

Of greatest importance is the effect of the contact resistance when different types of contact fluid are used. These ocasions arise when the thermal conductivity of a dry porous specimen is required; this usually means that the contact fluid is air which has a conductivity that is about 2 orders of magnitude less than that of fused silica. The contact resistance therefore becomes very important even when ℓ is small since $2\ell/\lambda_f$ may be large. Another common situation arises when the thermal conductivity is required of an oil bearing sediment in its natural state; with oil in the pores there is a tendency to use oil as the contact fluid. There is also a tendency to think that liquids have high conductivities; while it is true that they are significantly higher than for gases, a typical oil has a conductivity that is an order of magnitude less than that of fused silica. Table 4 shows some typical values of contact resistance for hard and soft rocks. Therefore, in these situations the experimental arrangement must be carefully examined for the possibility of systematic errors caused by ignoring these thermal contact resistances, and the first step is to find a way of determining the thickness of the equivalent film thickness ℓ. First equation (7) is recast into the form

$$(8)\quad D/2\ell = [1/\lambda_n]\,[1/\lambda_{no} - 1/\lambda_{nt}]^{-1}$$

where the subscript n refers to the parameters when the porous specimen is saturated with fluid n (e.g. n = air, or water, or oil etc.) which is also used as a contact fluid, λ_n is the conductivity of fluid n, D is the specimen thickness, λ_{no} is observed (apparent) conductivity of the specimen, and λ_{nt} is true conductivity of the specimen. If we could measure ℓ independently it would, ideally, be sensibly the same whichever fluid (n) is used. However, this cannot be done and it has to be found indirectly. For this we need a model that will allow the computation of a conductivity of specimen from its known composition; then ℓ can be determined since it is the only unknown in (8). If using two different fluids gives the same result for ℓ then we have reasonable confidence in the value for further measurements.

ℓ can be found if the apparent thermal conductivity is determined with two different fluids as saturants and contact medium but a valid model must be used for calculating the thermal conductivity of a porous material from a knowledge of its composition. Since we are dealing with a porous rock saturated with fluid, discussion will be confined to two component models. The physical picture is illustrated in Fig. 12 and Table (5) and shows some of the many mathematical models derived to match the situation in Fig. 12.

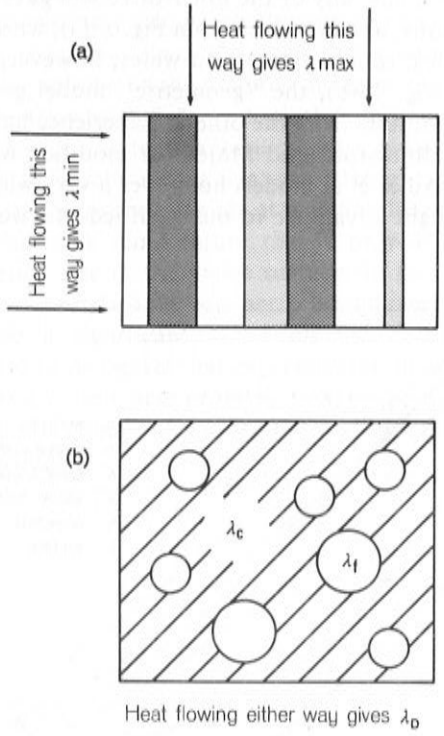

Figure 12. Schematic illustrating idealized arrangements of components in a multicomponent specimen: see also Table 5.

Table 5 – Two component models used for computing conductivities. ϕ = proportion (by volume) of discontinuous phase (= porosity for porous rocks), r = conductivity of continuous phase (matrix)/conductivity of discontinuous phase (voids) = λ_c/λ_v, X = (2r + 1), Y = (r – 1).

Model	Calculated Conductivity
1. Series (Minimum)	$\lambda_c/(\phi Y + 1)$
2. Parallel (Maximum)	$\lambda_c(r - \phi Y)/r$
3. Maxwell	$\lambda_c(X - 2\phi Y)/(X + \phi Y)$
4. Brailsford and Major (1964)	$\lambda_c[U + (U^2 + 8r)^{1/2}]/4r$ where $U = (2r - 1) - 3\phi Y$
5. Adler et al.(1973) (Parallel)	$\lambda_c[(\phi/\sqrt{r}) + (1 - \phi)]^2$
6. Weighted Geometric Mean	λ_c/r^{ϕ}

Although much used, the weighted geometric mean equation must be discarded since it has no physical basis, is purely empirical, and gives reasonable results only over a limited range of ∅ and r. In fact, over the range of r and ∅ for which the weighted geometric mean equation holds, any of the other three will gave equally good results, as can be seen from Fig. 13(a), where r = 5 — a typical ratio for rock and water; however, when r = 125, Fig. 13(b), the "geometric" model gives very different results from the others. Experience has shown that the Brailsford and Major (or modified Maxwell) and the Adler et al models hold over a very wide range with a slight advantage to the modified Maxwell.

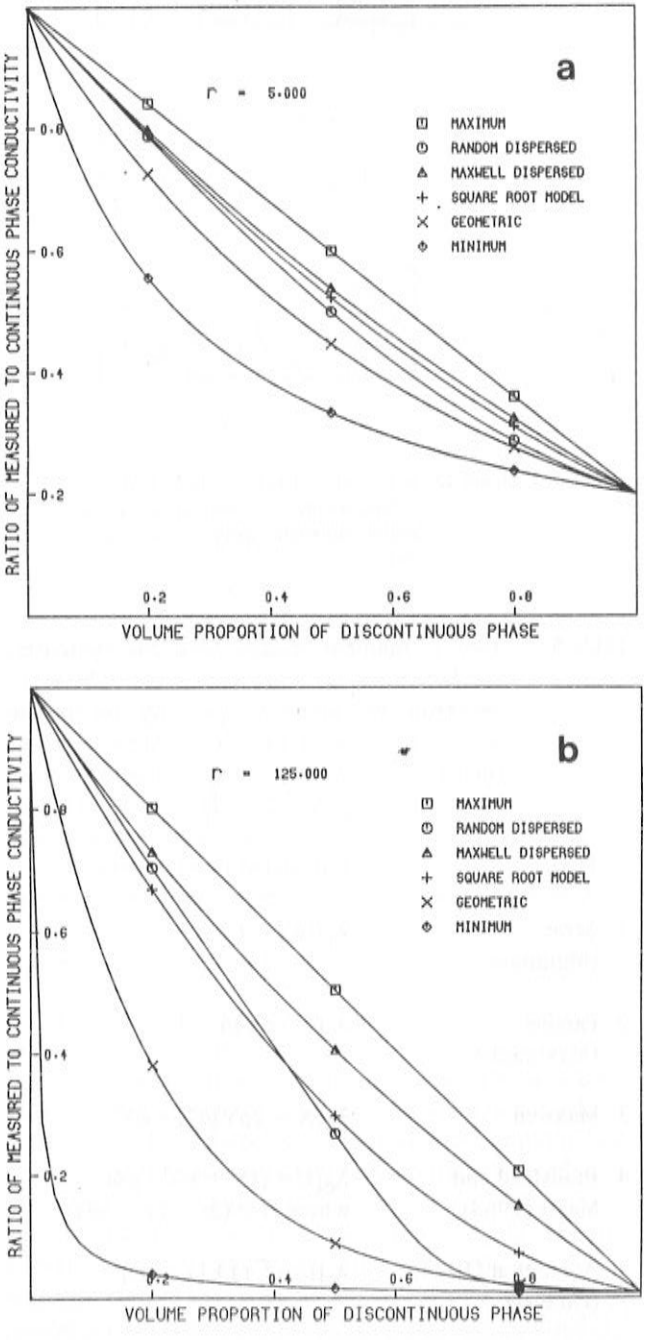

Figure 13. (a) Computed conductivities using models of Table 5 and r = 5. (b) As in (a) but r = 125.

The application of this approach can be demonstrated using data of Robertson & Peck (1974) who measured the conductivities of over 60 specimens of a single vesicular basalt; each specimen was characterized mineralogically and porosities ranged from 0.02 to 0.98. With a porosity of only 0.02 and filled with water, clearly we can find a good value for the matrix conductivity using any model. Robertson & Peck commented on the difficulty of getting the wet and dry values to make sense no matter which model was used. However, if we assume a significant thermal contact resistance for the dry state and go through the procedures mentioned earlier, the two sets of results are in good agreement if the thickness of the equivalent contact film is $\sim 10\mu m$.

As Table 6 shows, the equivalent filme thickness is consistent at 10 μm from specimen to specimen up to porosities of 35-40%. Now, this thickness is such that for the water filled contact the apparent thermal conductivity of a typical speciment would not be significantly different, at the 5% imprecision level, from the true thermal conductivity of the specimen, see Table 4; however, for an oil filled specimen and contacts, there would be a significant difference at the 15% level and a highly significant difference for specimens measured in the dry state.

Table 6 – Thickness (ℓ) of equivalent film of a vesicular basalt. Measured conductivity and porosity data taken from Robertson and Peck (1974). ϕ = porosity, λ_{wo} = measured conductivity when specimen is saturated with water, λ_m = derived matrix conductivity using model equation 4 of Table 5, λ_{ao} = measured conductivity when specimen saturated with air, λ_{at} = computed (true) air saturated conductivity using λ_m and model equation. Conductivities in W m^{-1} K^{-1}.

ϕ(%)	λ_{wo}	λ_m	λ_{ao}	λ_{at}	$\ell(\mu m)$
2	1.84	1.87	1.52	1.82	8
4	1.80	1.86	1.34	1.75	14
5	1.77	1.85	1.44	1.72	9
7	1.73	1.83	1.37	1.65	10
12	1.59	1.75	1.26	1.46	9
13	1.67	1.87	1.31	1.53	9
15	1.55	1.76	1.21	1.40	9
18	1.51	1.75	1.04	1.33	17
19	1.52	1.78	1.16	1.33	8
28	1.39	1.77	0.99	1.13	10
32	1.28	1.68	0.87	1.00	11
35	1.23	1.64	0.89	0.92	3

Clearly ignoring such effects can lead to considerable systematic error. Ideally, we should revert the original but more time consuming approach of using three or more disks of different thickness cut from the same material; unfortunately, even if time is not a

problem it is sometimes not possible to do this because of a lack of sufficient material.

Transient (Needle Probe) Methods

We now examine some sources of error in the "needle probe" technique which are likely to occur if the experiments are hastily designed. As is well known, for a perfectly conducting probe with heat supplied at a rate of Q per unit lenght per unit time and assuming no axial heat losses, the temperature rise $\theta(t)$ after time t is given by

$$(9)\quad \theta(t) = (Q/4\pi\lambda)\{2h-(2h-B)/(2B\gamma)+[1-((B-1)/2B\gamma)]\ell n\, Dt+\ldots\}$$

where $h = \lambda/(aC_y)$ is a dimensionless contact resistance parameter, $\gamma = \alpha t/a^2$ is a dimensionless time parameter, $B = (\varrho C)_{material}/(\varrho C)_{probe}$, $D = 4\alpha/a^2 \exp(g)$, a = probe radius, g = 0.5772 and is Euler's constant, α = thermal diffusitivy, λ = thermal conductivity, C_y = thermal conductance per unit length of the contact layer at r = a.

For sufficiently large γ, which essentially means that $a^2 << \alpha t$, the higher order terms can be ignored and, provided the experimental time is also large enough for h to be ignored, the conductivity is given by the familiar line source equation

$$(10)\quad \theta(t) = (Q/4\pi\lambda)\,\ell n\, t + S$$

where $S = (Q/4\pi\lambda)(2h + \ell nD)$. This equation holds for all time provided that the regime is purely conductive and that no far boundary effects occur.

The first problem is that, contrary to a number of misconceptions, probe measurements also introduce a thermal contact resistance at the boundary between the probe and the material (see Fig. 7). In fact, if considerable care and thought is not exercised one of the great advantages of the needle probe technique may lead to a source of significant error. The needle probe technique is used widely for measuring the thermal conductivity of sediments and its big advantage is that results can be obtained quite quickly — in two or three minutes under proper experimental conditions — so that many measurements can be made along the length of an oceanic or lake bottom core. In general, the smaller the radius of the probe, the shorter the time rquired to arrive at the region of the logarithmic asymptote and hence the more quickly the set of measurements can be obtained. Fig. 14 shows a typical temperature — time plot for a large radius (1-5 cm) probe; for a needle probe (radius = 0.5-1 mm) the time units would change from minutes to seconds. However, if ever shorter times of measurement are sought by decreasing the radius of the probe, situations may arise where the radius of the grains of the sedimentary material is so large compared to the radius of the probe that the principal contribution to the result comes from the thermal property of the saturating and contact medium. This is because as a transient method, the depth of penetration of heat into the medium is a function of time, as well as the thermal properties of a small cylinder of the medium; for a short term experiment, one is essentially measuring the thermal properties of the material close to the probe boundary. If the experiment is run for a long time, the particular nature of the material near the boundaries becomes less and less important since it is averaged in with an ever increasing volume of the material at larger radii. It can easily be shown, that for a typical experiment lasting three minutes, the temperature rise at a radial distance of twice the probe radius is about 80% of that at the surface of the probe whereas at a radial distance of 50 probe radii the temperature rise is only 1% of the temperature rise at the probe surface. In fact, for r > 50a, the material could be a perfect conductor and still not have a significant effect on the results. It is important to recognize that experimental times that are too short give only near probe thermal properties; larger experimental times average the thermal properties over a large volume.

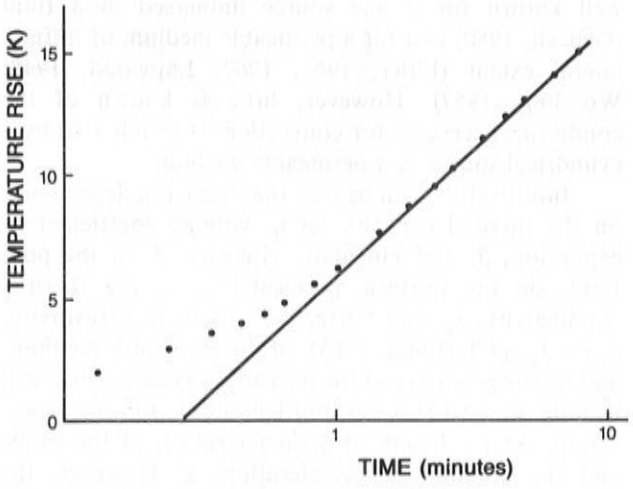

Figure 14. Temperature-time (on a log scale) plot for a probe experiment, probe radius 1-5 cm; for a needle probe (radius 0.5-1mm) time scale changes to seconds.

The second problem arises from the fact that the "needle probe" technique is widely used on unconsolidated sediments, especially oceanic and lake bottom sediments, which may have porosities as high as 0.7. With such high porosities it is inevitable that high permeabilities also occur and there is a very real danger of convection being induced in the experiment unless great care is taken in the experimental design.

It follows from the line source equation that if we are on the asymptotic portion of the plot then equation 10 can be rewritten to read

$$(11)\quad \lambda_{t_n} = (Q/4\pi)[\ell n(t_{n+1}/t_n)]/[\theta_{n+1} - \theta_n]$$

where $(\theta_{n+1} - \theta_n)$ is the incremental temperature rise over the time incremen Δt from time t_n. If the experimental conditions match the boundary conditions required by theory then the value of the thermal conductivity should be independent of time. On the other hand, if the approximation is incorrect, either

because some of the terms which have been ignored are in fact significant (e.g. there is a contact resistance) or because some other forms of heat transfer occur (e.g. convection), then the apparent thermal conductivity will be a function of time.

Even though the temperature rise in a line source experiment may be only a few degrees, the temperature gradient near the probe is one or two orders of magnitude higher than the gradient elsewhere away from the probe, or than the gradient across a disk in a typical divided bar experiment. It therefore follows that there is a much higher probably that the temperature gradient will exceed the critical gradient near the probe surface and induce convection in a probe experiment.

In general, convection occurs when the buoyancy forces exceed the gravitational forces but the theoretical relationships among the various parameters involved depends on the geometry of the system being investigated. The conditions for onset of free convection in a borehole are well known (Hales, 1937), essentially a one-dimensional problem. They are also well known for a line source immersed in a fluid (Genceli, 1980) and for a permeable medium of infinite lateral extent (Elder, 1965, 1967; Lapwood, 1948; Wooding, 1957). However, little is known of the conditions necessary for convection to be initiated by a cylindrical source in a permeable medium.

Intuitively, it can be seen that there is a dependence on the thermal capacity $(\varrho C)_f$, volume coefficient of expansion, β, and kinematic viscosity, ϑ, of the pore fluid; on the intrinsic permeability, k, the thermal conductivity, λ_s, and "effective" thermal diffusitivity, α_e ($= \lambda_s/(\varrho C)_f$ (Elder, 1965), of the permeable medium: and on the geometry of the measuring system which will include the heat flux per unit length, Q, and the aspect ration, A* (= length to diameter ratio), of the probe and the gravitational acceleration, g. However, the theoretical relationship among these parameters for the onset of convection is difficult to determine.

In a series of experiments, Fodomesi & Beck (1983) have investigated the conditions under which convection can occur and derived an empirical convection parameter which they proposed should be used in the design of probe experiments to avoid induced convection even in highly permeable materials.

Convection occurs most readily when the gravitational forces (and the buoyancy forces and therefore the temperature gradient) are parallel to each other; when the temperature gradient is orthogonal to the gravitational field then the onset of convection is significantly inhibited. Since in the probe experiment the temperature gradient is radial, if there are convection effects present there should be differences in the experimental results according to whether the axis of the experiment is horizontal or vertical; therefore one variable introduced into the experimental design was the orientation of the axis of probe.

To minimize the number of variables in such a complex experiment, artificial media were created using glass beads of different diameters but of the same composition; furthermore, these were packed in similar fashion so that all media had the same porosity. However, because of the different diameters the intrinsic permeabilities ranged from $9x10^{-8}$ to $2x10^{5}$ cm^2. Thus all media had the same matrix conductivity, the same porosity, but different permeabilities.

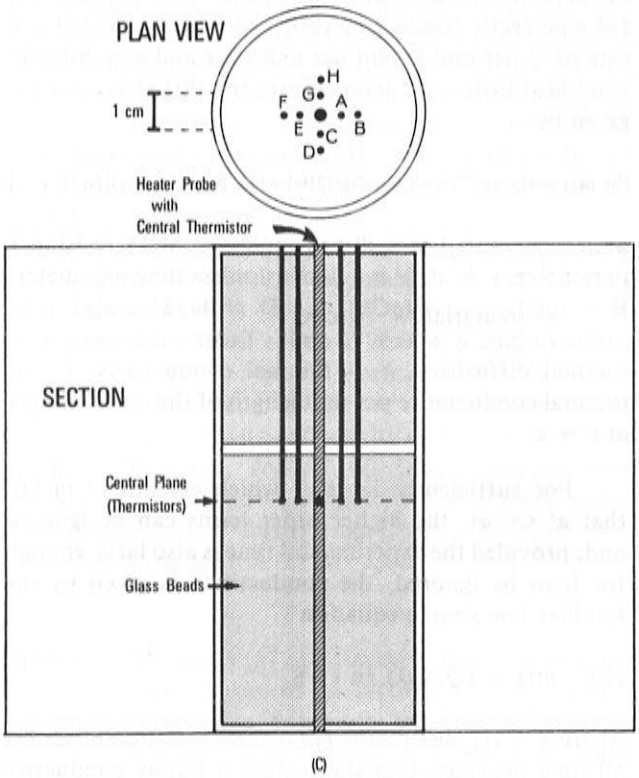

Figure 15. Schematic of arrangement for induced convection experiments in needle probe apparatus.

The experimental set-up is shown in Fig. 15. In addition to the usual temperature sensor at the geometric centre of the needle probe, eight other sensors are located at 5mm and 10mm radii on orthogonal diameters (Figure 15(a)) through the central plane, (Fig. 15(b)); these are placed there to make the direction of the onset of convection easier. If there is no convection the temperature rises on all the sensors at r = 5mm should be identical, but lower than the probe temperature rise, and the temperature rises for all sensors at r = 10mm should also be identical, but less than those at r = 5mm/ furthermore, the temperature differences between the pairs of sensors at r = 5mm and r = 10mm on one radial should be the same as the differences on all other radials. If convection occurs then there will be departures from these conditions.

Fig. 16 shows some typical results for water saturated media, the temperature rises and differences being normalized to the power input. It can be seen from (a), (b) and (c) that when the probe axis is vertical and the radial temperature gradient is therefore always orthogonal to the gravitational field, there is no indication of convection. The apparent conductivity, equation 11, is constant from 10 to 1,000 seconds

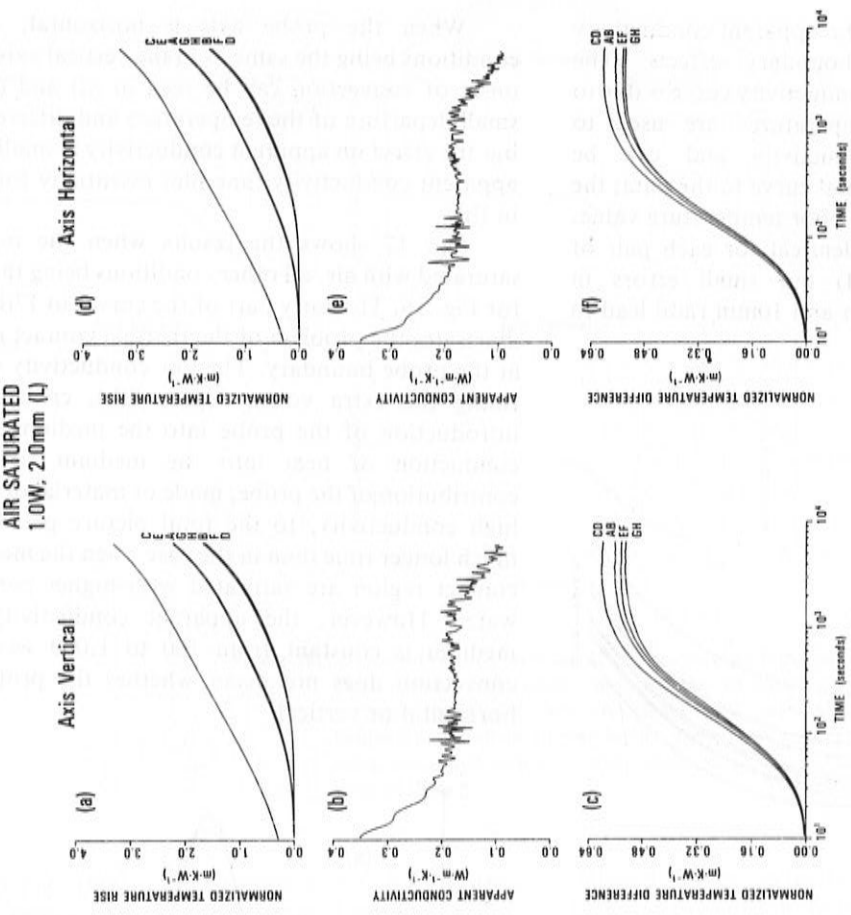

Figure 17. Similar to Figure 16 but air saturated case. Note contact resistance effect in (b) and (e) lasting for 100 seconds; see text.

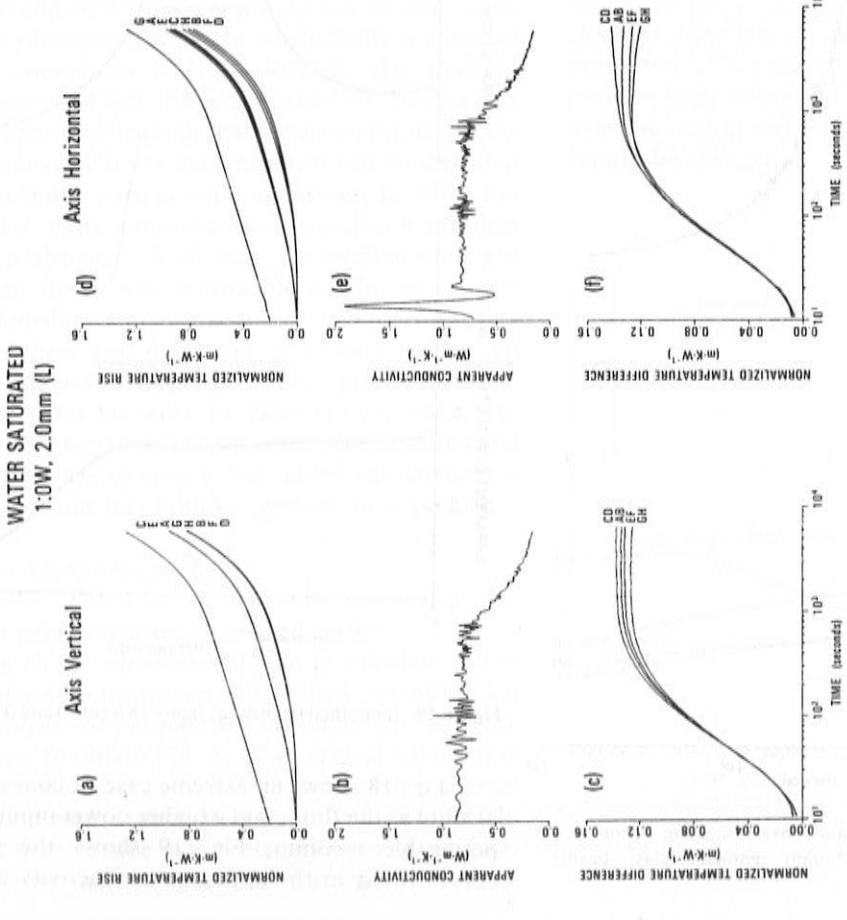

Figure 16. Unprocessed results for some experiments using 2mm diameter glass beads and power input of 2W to a 15cm long probe of 3mm diameter. Temperature rises and differences are normalized to the power input (see equation 10). No convection evident in vertical axis case; convection just evident in (d) and (f).

although after 1,000 seconds the apparent conductivity decreases because of far boundary effects. The "spikeness" of the apparent conductivity curve is due to the fact that successive temperatures are used to calculate the apparent conductivity and can be smoothed by fitting a polynomial curve to the data; the large spike in (e) is due to one poor temperature value. In (c) the curves should be identical for each pair of sensors (CD, AB, EF, GH) but small errors in positioning the sensors at 5mm and 10mm radii lead to systematic differences.

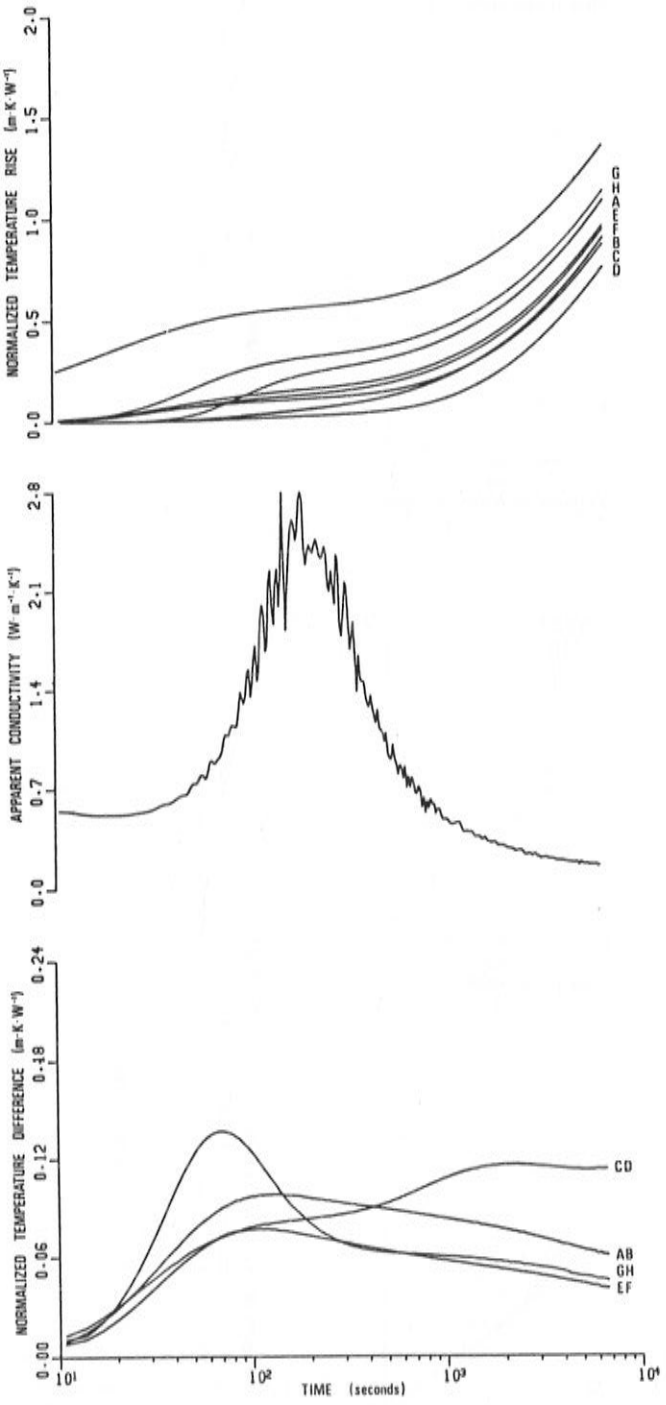

Figure 18. Example for very significant convection using alcohol as a fluid in medium of 3mmm diameter glass beads; unprocessed records.

When the probe axis is horizontal, all other conditions being the same as in the vertical axis case, the onset of convection can be seen in (d) and (f) by the small departure of the temperature and difference plots but the effect on apparent conductivity is small since the apparent conductivity-time plot essentially follows that in (b).

Fig. 17 shows the results when the medium is saturated with air, all other conditions being the same as for Fig. 16. The early part of the curves in 17(b) and (e) illustrates the problem of the thermal contact resistance at the probe boundary. The low conductivity of the air filling the extra voids, Figure 8(b), created by the introduction of the probe into the medium slows the conduction of heat into the medium so that the contribution of the probe, made of material or relatively high conductivity, to the total picture persists for a much longer time than in the case when the medium and contact region are saturated with higher conductivity water. However, the apparent conductivity of the medium is constant from 100 to 1,000 seconds and convection does not occur whether the probe axis is horizontal or vertical.

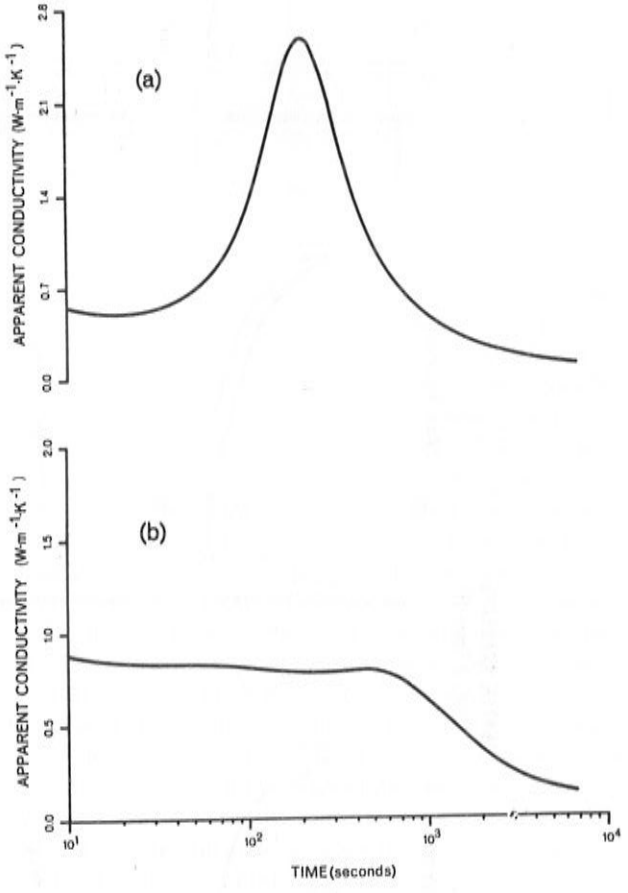

Figure 19. Smoothed records (a) figure 18 (centre) and (b) figure 16(e).

Fig. 18 shows an extreme case of convection using alcohol as the fluid, and a higher power input in a highly permeable medium; Fig. 19 shows the polynomial curves fitted to the apparent conductivity plot of Fig.

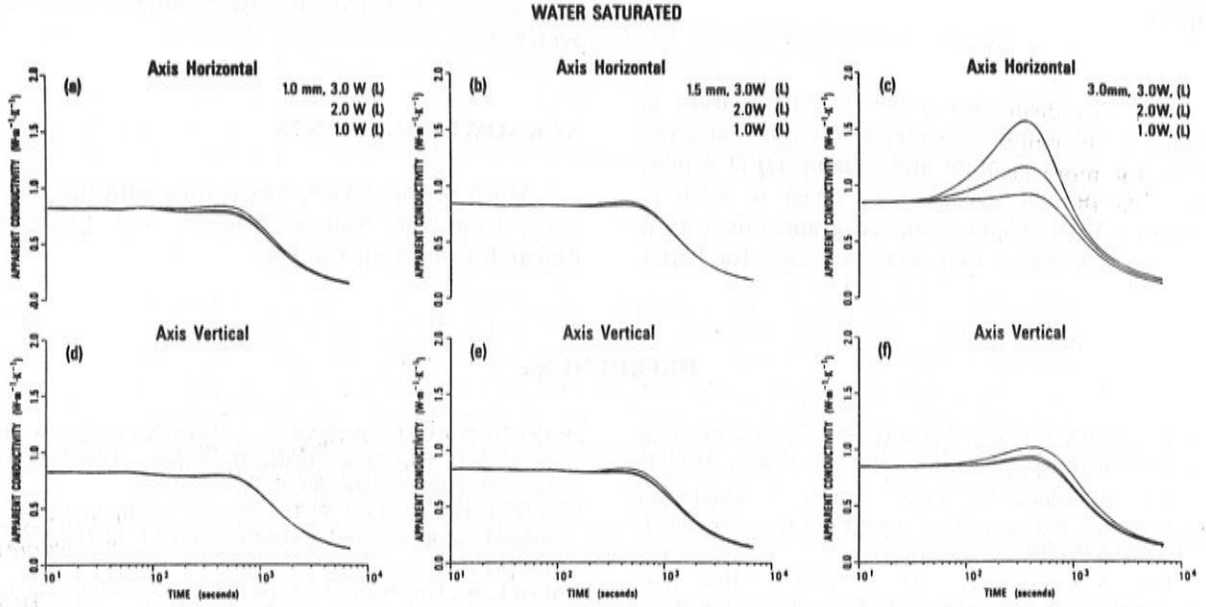

Figure 20. Smoothed records showing differences between horizontal and vertical axis cases, and effects of increasing permeability (from left to right) and increasing temperature gradient (power input), the largest gradient being associated with top curve, where separable, in the suite of three.

18(b) and Fig. 16(e). Fig. 20 summarizes the situation for water saturated media using 1mm, 1,5mm and 3mm diameter glass beads (i.e. variable intrinsic permeability) and using 1, 2 and 3 watt inputs to the heater for the horizontal and vertical axis cases. As can be seen, when the axis is vertical the apparent conductivity is constant in most cases from 10-1,000 seconds; the onset of convection can be seen in Fig. 20(c) and (f). For the case when the axis is horizontal, that is the conditions for the onset of convection are maximized, it can be seen that for 1 watt input there is not a significant problem but for 2 and 3 watts input there is a significant problem when the probe axis is horizontal. Convection could not be induced under any reasonable conditions for air saturated media.

From these and numerous other experiments, an empirical dimensionless parameter Φ, equation (12), can be derived from the work of Elder (1967), which will allow us to specify ahead of time the experimental conditions needed to ensure that the critical gradient is not exceeded and that induced convection is avoided.

$$(12) \quad \Phi = k\beta g Q A^* 5 a_e^2 \nu (\varrho C)_f$$

where the parameters are as defined earlier.

Using all the experimental data to calculate values of the convection parameter, Φ is plotted versus the log of the ratio of apparent conductivity to true conductivity to obtain Fig. 21. Two critical values of Φ can be seen such that provided we choose experimental conditions to ensure that Φ does not exceed about 900 in the case for the probe axis horizontal and about 1500 for the probe axis vertical, convection will not be induced. To be perfectly safe Φ should be less than 900 under any condition. In practice the only parameter that can be varied is the power input because $(\varrho C)_f$, β and ν are the properties of the saturating fluid, K, a_e and λ_s are the properties of the saturated medium and cannot be changed if the laboratory measurements are to give the properties of a specimen of natural material; the A* must be large enough to guarantee one radial heat flow over the central section of the cylindrical system, and g cannot be changed.

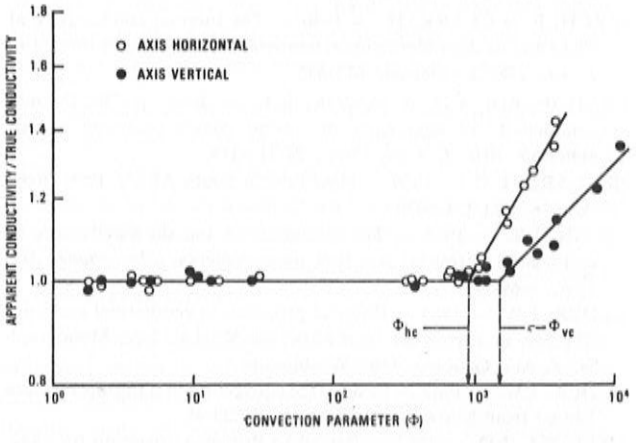

Figure 21. Plot of apparent conductivity/true conductivity ratio versus convection parameter (Φ), on a log scale; see equation (11) and text. Note critical values of Φ at about 950 (horizontal axis) and 1800 (vertical axis) above which convection sets in with vigorousness increasing with increasing Φ

SUMMARY

This paper has dealt with a few problems areas in geothermics, the common theme of which is that given the need for more accurate and reliable HFD values, considerable thought needs to be given to what is required of a field or laboratory program; this in turn leads to the conclusion that there is a case for better experimental design if the desired objectives are to be achieved.

ACKNOWLEDGEMENTS

Much of this review was written with the aid of a grant from the Natural Sciences and Engineering Research Council of Canada.

REFERENCES

ADLER, D., FLORA, L.P. & SENTURA, S.D. — 1973 — Electrical conductivity in disordered systems, *Solid State Comm.*, **12**:9-12.

ALLIS, R.G. & GARLAND, G.D. — 1976 — Geothermal measurements in five small lakes in northwest Ontario. *Can. J. Earth Sci.*, **13**:987-992.

ALLIS, R.G. & GARLAND, G.D. — 1979 — Heat flow measurements under some lakes in the Superior Province of the Canadian Shield. *Can. J. Earth Sci.*, **16**:1951-1964.

BECK, A.E. — 1957 — A steady state method for the rapid measurement of the thermal conductivity of rocks, *J. Sci. Instr.*, **34**:186-189.

BECK, A.E. — 1977a — Climatically perturbed temperature gradients and their effect on regional and continental heat-flow means, *Tectonophysics*, **41**:17-39.

BECK, A.E. — 1977b — A potential systematic erro when measuring the thermal conductivity of porous rocks saturated with a low conductivitv fluid, *Tectonophysics*, **41**:9-16.

BECK, A.E. — 1980 — Heat flow measurements under some lakes in the Superior province of the Canadian Shield: Discussion, *Can. J. Earth Sci.*, **17**:1108-1110.

BECK, A.E. — 1982 — Precision logging of temperature gradients and the extraction of past climate. *Tectonophysics*, **83**:1-11.

BECK, A.E., ANGLIN, F.A. & SASS, J.H. — 1971 — Analysis ofheat flow data: in situ thermal conductivity measurements, *Can. J. Earth Sci.*, **8**:1-19.

BECK, A.E., JAEGER, J.C. & NEWSTEAD, G.N. — 1956 — Thew measurement of thermal conductivities of rocks by observations in boreholes, *Austral. J. Phys.*, **9**:286-296.

BENFIELD, A.E. — 1939 — Terrestrial heat flow in Great Britain *Proc. Roy. Soc.*, **173**:428-450.

BIRCH, F. & CLARK, H. — 1940 — The thermal conductivity of rocks and its dependence upon temperature and composition, *Am. J. Sci.*, **238**:529-558, and 613-635.

BRAILSFORD, A.D. & MAJOR, K.F. — 1964 — The thermal conductivitv of aggregates of several phases including porous materials, *Brit. J. Appl. Phys.*, **15**:313-319.

BULLARD, E.C. — 1939 — Heat flow in South Africa, Proc. Roy. Soc. A, **173**:474-502.

CRAIN, I.K. — 1968 — The glacial effect and the significance of continental terrestrial heat flow measurements, *Earth Planet. Sci. Lett.*, **4**:69-72.

ELDER, J.W. — 1965 — Physical processes in geothermal areas,pp. 211-239, in *Terrestrial Heat Flow*, ed. W.H.K. Lee, Monograph Nº 8, Am. Geophys. Un., Washington.

ELDER, J.W. — 1967 — Steady free convection in a porous medium heated from below, *J. Fluid Mech.*, **27**:29-48.

EVERETT, J.D. — 1883 — Report to British Association for 1882, 72-90.

FINCKH, P. — 1981 — Heat flow measurement in 17 perialpine lakes. *Geol. Soc. Am. Bull. Part II*, **92**:452-514.

FODEMESI, S.P. & BECK A.E. — 1983 — Induced convection during cylindrical probe conductivity measurements, pp. 619-634, in *Thermal Conductivity*, **17**, ed. J.G. Hust, Plenum, N.Y.

FRANCHETEAU, J., JAUPART, C., SHEN, X., KANG, W., LEE, D., BAI, J., WEI, H. & DENG., H. — 1984 — High heat flow in southern Tibet, *Nature*, **307**:32-36.

GENCELI, O.F. — 1980 — The onset of manifest convection in suddnely heated horizontal cylinders, *Warme u. Stoffubertragung*, **13**: 163-169.

HAENEL, R., GRONLIE, G. & HEIER, K.S. — 1974 — Terretrial heat flow determinations from lakes in Southern Norway, *Norsk Geologisk Tidskrift*, **54**:423-428.

HALES, A.L. — 1937 — Convection current in geysers, *Monthly Nat. Roy. Astr. Soc. Geophys. Suppl.*, **4**:122-131.

HANSEN, B.L. & LANGWAY, C.C. — 1966 — Deep core drilling in ice and core analysis at Camp Century, Greenland, 1961-66, *Antarctic J.U.S.*, **1**:207-208.

HART, S.R. & STEINHART, J.S. — 1965 — Terrestrial heat flow: measurement in lake bottoms. *Science*, **149**:1499-1501.

JAUPART, C., FRANCHETEAU, J. & SHEN, X. — 1985 — On the thermal structure of the southern Tibetan crust, *Geophys. J. Roy. Astr. Soc.* **81**:131-155.

KRIGE, L.J. — 1939 — Borehole temperatures in the Transvaal and Orange Free State, *Proc. Roy. Soc. A*, **173**:450-474.

LAPWOOD, E.R. — 1948 — Convection of a fluid in a porous medium, *Proc. Cam. Phil. Soc.*, **44**:508-521.

LINDQVIST, J.G. — 1984 — Heat flow density measurements in the sediments of three lakes in northern Sweden, *Tectonophysics*, **103**: 121-140.

MAIRAN, J.J.D. — 1749 — Dissertation sur la glace on explication physique on la formation de la glace et de ses divers phenomenes, *L'Imprimerie Royale*, Paris.

NIELSEN, S.B. — 1986 — The continuous temperature log: method and applications, Ph.D. tesis, University of Western Ontario, London, Ontario, Canada.

POWELL, W.G., CHAPMAN, D.S., BALLING. N. & BECK A.E. — 1987 — Continental heat flow density in *Monograph on Geotermics*, eds. L. Rybach, L. Stegena, R. Haenel, Reidel.

ROBERTSON, E.C. & PECK, D.L. — 1974 — Thermal conductivity of vesicular basalt from Hawaii, *J. Geophys. Res.*, **79**:4875-4888.

STRAUSS, J.M. & SCHUBERT, J. — 1977 — Thermal convection in a porous medium: effects of temperature and pressure-dependent thermodynamic and transport properties, *J.Geophys. Res.*, **82**:325-333.

VILLINGER, H. — 1983 — In situ bestimmung der warmeleitfahigkeit in bohrungen, Ph.D. thesis, Tech. U. Berlin.

VON HERZEN, R.P. & MAXWELL, A.E. — 1959 — The measurement of thermal conductivity of deep sea sediments by a needle-probe method, *J. Geophys. Res.*, **64**:1557-1563.

WANG, K. & BECK, A.E. — 1987 — Heat flow measurement in lacustrine or oceanic sediments without recording bottom temperature variation *J. Geophys. Res.*, **92**:12837-12845.

WANG, K., SHEN, P.Y. & BECK, A.E. — 1986 — On the effects of thermal properties structure and water bottom temperature variation on temperature gradients in lake sediments, *Can. J. Earth Sci.*, **23**:1257-1264.

WOODING, R.A. — 1957 — Steady state free thermal convection of liquid in a saturated permeable medium, *J.Fluid. Mech.*, **2**:273-285.